Holographic coherent states from random tensor networks

Xiao-Liang Qi,[a] **Zhao Yang**[a] **and Yi-Zhuang You**[b]

[a]*Department of Physics, Stanford University,*
Stanford, CA 94305, U.S.A.

[b]*Department of Physics, Harvard University,*
Cambridge, MA 02138, U.S.A.

E-mail: xlqi@stanford.edu, zhaoyang@stanford.edu, yiy808@g.harvard.edu

ABSTRACT: Random tensor networks provide useful models that incorporate various important features of holographic duality. A tensor network is usually defined for a fixed graph geometry specified by the connection of tensors. In this paper, we generalize the random tensor network approach to allow quantum superposition of different spatial geometries. We setup a framework in which all possible bulk spatial geometries, characterized by weighted adjacent matrices of all possible graphs, are mapped to the boundary Hilbert space and form an overcomplete basis of the boundary. We name such an overcomplete basis as holographic coherent states. A generic boundary state can be expanded in this basis, which describes the state as a superposition of different spatial geometries in the bulk. We discuss how to define distinct classical geometries and small fluctuations around them. We show that small fluctuations around classical geometries define "code subspaces" which are mapped to the boundary Hilbert space isometrically with quantum error correction properties. In addition, we also show that the overlap between different geometries is suppressed exponentially as a function of the geometrical difference between the two geometries. The geometrical difference is measured in an area law fashion, which is a manifestation of the holographic nature of the states considered.

Contents

1 Introduction

The holographic duality [1–3] was proposed as a duality between quantum gravity in $d+1$ dimensions and quantum field theory in d dimensions. The correspondence was originally proposed between the partition function and correlation functions of the two theories. The large N limit of the boundary quantum field theory corresponds to the bulk semiclassical limit (the limit of small Newton constant G_N). The role of quantum entanglement in holographic duality was explicitly reflected by the Ryu-Takayanagi formula [4] and its generalizations [5–8], which relates entanglement entropy of a boundary region to area of extremal surfaces. The relation of entropy and area motivated the proposal that tensor networks may provide a "microscopic" framework for understanding holographic duality [9, 10]. Tensor networks, or projected entangled pair states (PEPS) is an approach to construct entangled quantum many-body states [11–16]. For a graph (see figure 1), the corresponding PEPS is obtained by first preparing an EPR pair for each link, and then projecting all qubits at the same vertex to a pure state specified by the tensor at that vertex. This procedure leads to a many-body state of the remaining qubits living at the end of dangling legs of the network. The advantage of the tensor network description is that the entanglement structure of the state is encoded explicitly in the geometry of the network. In particular,
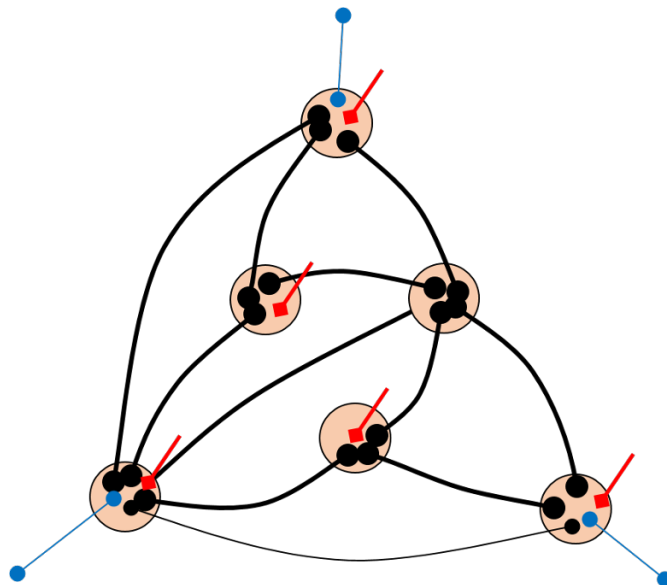
Figure 1. An example of random tensor network.

the entanglement entropy of each region A is bounded by the minimal number of links that separate A and its complement, multiplied by $\log D$ with D the bond dimension of each tensor. This is the analog of RT formula.

To use tensor networks to understand holographic duality, a key question is what states correspond to semiclassical bulk geometry. As we learn in holographic duality, such states must satisfy various conditions [17, 18], such as the negative tripartite mutual information [19]. Various tensor network models [20–23] have been proposed to incorporate desired features of holographic duality. Among them, the random tensor networks [23] are shown to realize many features of holographic duality naturally, including the RT formula with quantum corrections, and the quantum error correction property of the bulk-boundary holographic mapping [24]. However, there are holographic properties that are not reproduced by tensor networks, such as the Renyi entropy behavior [8, 25]. There are also obviously many other open questions that have not been addressed in the tensor network framework.

Among the open questions, an essential one is how to describe quantum superposition of different geometries, as is required for a quantum gravity theory. This is also a necessary step towards understanding Einstein equation and graviton excitations in the bulk. In this paper we make a small progress along this direction by setting up a framework for describing quantum superposition of tensor network states on arbitrary geometries. We generalize the random tensor network approach in ref. [23] and define a linear map between geometries in the bulk and quantum states on the boundary. A geometry is described by the adjacient matrix a_{xy} of a weighted (unoriented) graph (with fixed number of vertices and arbitrary connectivity), which is defined as a basis vector $|\{a_{xy}\}\rangle$ in the bulk. The linear map defined by random tensors then maps each such basis state to a quantum state $|\Psi\left[\{a_{xy}\}\right]\rangle$ on the boundary, which is the holographic state that is dual to this geometry. With this linear map

it is straightforward to take superpositions between different geometries. We prove that for a fixed size of the boundary, a large enough number of bulk vertices make such a mapping an isometry from the boundary to the bulk. In other words, $|\Psi\left[\{a_{xy}\}\right]\rangle$ parameterized by the weighted adjacent matrix a_{xy} form an overcomplete basis of the boundary, such that each state in the boundary Hilbert space can be mapped to a quantum superposition of different geometries. Due to the analog of boson coherent states (as will be elaborated more in later part of this paper), we name this basis of states "holographic coherent states".

Furthermore, this formalism allow us to consider small fluctuation around a classical geometry, and show that such small fluctuations for a "code subspace"[24] which is mapped to the boundary isometrically. (The precise meaning of "classical geometry" and "small fluctuation" will be given later. In short, a classical geometry means all nonzero entries of the weighted adjacent matrix a_{xy} are large, while small fluctuations correspond to $a_{xy} \to a_{xy} + \delta a_{xy}$ with $\delta a_{xy} \ll a_{xy}$.) Such small fluctuations can be considered as low energy states of the bulk quantum fields. The existence of bulk-boundary isometry in such subspaces guarantees that small fluctuations at different links of the graph are independent physical degrees of freedom. In other words, bulk locality emerges in such subspaces even if the whole bulk theory is intrinsically nonlocal. In addition, the bulk-boundary isometry satisfies the local reconstruction properties known in holographic duality. The structure of a boundary-to-bulk isometry in the whole boundary Hilbert space and a bulk-to-boundary isometry in code subspaces has been proposed as "bidirectional holographic code" in ref. [22], which is schematically summarized in figure 2.

As an overcomplete basis, states $|\Psi\left[\{a_{xy}\}\right]\rangle$ for different geometry a_{xy} do not correspond to orthogonal states of the boundary. However, we show that the overlap between different geometries are exponentially suppressed in the large N limit. This is similar to ordinary boson coherent states that are used in mean-field approximation of superfluids and superconductors. Different coherent states are not orthogonal. But because their overlap is exponentially small, it is physically meaningful to consider them as physically different states, and therefore consider the condensate wavefunction as a physical order parameter field. An interesting difference of the geometrical states from ordinary coherent states is that the overlap between two states has a "holographic" behavior. If two geometries a_{xy} and b_{xy} are distinct in a region R and identical outside R, we prove that the overlap $|\langle \Psi\left[\{a_{xy}\}\right]|\,\Psi\left[\{b_{xy}\}\right]\rangle|$ is upper bounded by $e^{-c|\gamma|}$ with γ the area of a minimal surface bounding region R. c is a constant determined by the entanglement entropy contributed by each link crossing the boundary. The area law form of the overlap is a manifestation of the fact that the states $|\Psi\left[\{a_{xy}\}\right]\rangle$ are consistent with the holographic principle — the fact that the physical degrees of freedom in a region R are bounded by their area rather than volume.

The remainder of the article is organized as follows. In section 2 we present the general setup of our approach. In section 3 we study the condition of boundary-to-bulk isometry. In section 4 we investigate the definition of classical geometries and the code subspaces with bulk-to-boundary isometry. In section 5 we study the overlap between different classical geometries to show that distinct geometries are almost orthogonal. Finally, the conclusion and further discussions are given in section 6.
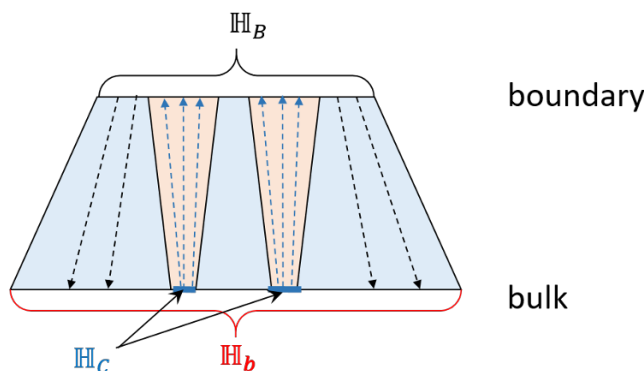
Figure 2. Illustration of the structure of bidirectional holographic code defined by RTN. An isometry is defined from the boundary Hilbert space $\mathbb{H}_B$ to bulk Hilbert space $\mathbb{H}_b$ which maps each state in $\mathbb{H}_B$ to a superposition of geometries. In the code subspace $\mathbb{H}_C$ which consists of subspaces of small fluctuations around different classical geometries, an isometry is defined from bulk to boundary.

2 General framework

We begin with a brief overview of the random tensor networks proposed in ref. [23]. For a graph, such as the one in figure 1, one first prepares a EPR pair of two qudits for each link, denoted by $|xy\rangle$. Then the RTN is defined by projecting all qudits on the site x to a random pure state $|V_x\rangle$. If each qudit has dimension D, and site x has k neighbors, $|V_x\rangle$ is a random unit vector in a D^k-dimensional Hilbert space. The probability distribution of $|V_x\rangle$ is uniform, which means $|V_x\rangle$ and $U|V_x\rangle$ has the same probability for any unitary U. Alternatively, one can define $|V_x\rangle = U|0\rangle$ with U a Haar random unitary operator and $|0\rangle$ a fixed reference state. For a graph G, the RTN state is expressed as

$$|\Psi_G\rangle = \prod_x \langle V_x| \prod_{\langle xy\rangle \in G} |xy\rangle \tag{2.1}$$

with the $\langle xy\rangle \in G$ runs over (unoriented) edges in the graph G.

From the definition of RTN, it is natural to see how to generalize this formalism to include superposition of different geometries (graphs)—The link state $\prod_{\langle xy\rangle \in G} |xy\rangle$ can be replaced by superpositions of such states on different graphs. To make this well-defined, one needs to modify the definition slightly to make sure the Hilbert space dimension of each vertex is identical for different graphs. This can be easily achieved by defining some auxiliary states on links that are absent in G. For each $\langle xy\rangle \notin G$, define a state $|xy\rangle_0 = |x\rangle_0 |y\rangle_0$ which is a direct product state and is orthogonal to $|xy\rangle$. Adding such direct product states do not change the entanglement structure of the system. Then if we replace $\prod_{\langle xy\rangle \in G} |xy\rangle$ by $\prod_{\langle xy\rangle \in G} |xy\rangle \prod_{\langle xy\rangle \notin G} |xy\rangle_0$, the dimension of each site is D^{V-1} if the total number of vertices is V. Therefore the random states $|V_x\rangle$ can be chosen in a Hilbert space of dimension D^{V-1} independent from G. Denote $|P_G\rangle = \prod_{\langle xy\rangle \in G} |xy\rangle \prod_{\langle xy\rangle \notin G} |xy\rangle_0$ as the "parent state" before projection, then the superposition of two geometries G, G' correspond to a boundary state $a|\Psi_G\rangle + b|\Psi_{G'}\rangle = \prod_x \langle V_x| [a|P_G\rangle + b|P_{G'}\rangle]$. In other
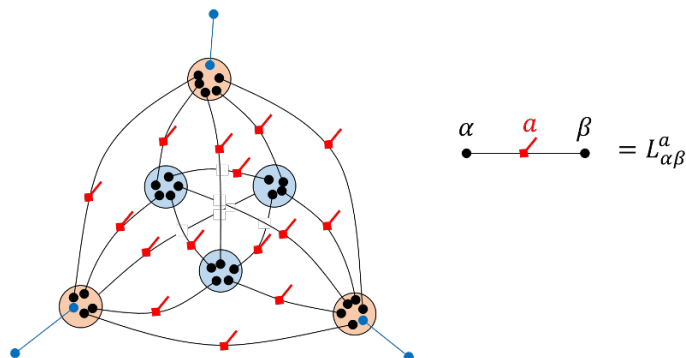
Figure 3. Illustration of the random tensor network on a complete graph with link states. Each bulk link is a three-leg tensor $L^a_{\alpha\beta}$, and each vertex is a random tensor. The blue links are maximally entangled EPR pairs. The network defines a linear map between bulk link states (red lines) and boundary states (blue lines).

words, now we have a *linear map* between different graphs G corresponding to different EPR pair configurations (in the *same* Hilbert space) to different boundary states.

Motivated by the discussion above, we consider a more general situation and define the following tensor network. Consider a complete graph with V vertices, in which V_B of them are labeled as "boundary" vertices, and the rest of them $V_b = V - V_B$ are bulk vertices. For each pair of vertices x, y ($x \neq y$), we define a three-leg tensor $L^{\alpha\beta}_a$ shown in figure 3, with $a = 0, 1, 2, \ldots, D_L - 1$ and $\alpha, \beta = 1, 2, \ldots, D$.[1] This tensor defines an isometry from index a to indices $\alpha\beta$. In other words, states

$$|a_{xy}\rangle = L^{\alpha\beta}_a |\alpha\rangle_x |\beta\rangle_y \tag{2.2}$$

are orthonormal, i.e. $\langle b_{xy} | a_{xy} \rangle = \delta_{ab}$. (Obviously this requires $D_L \leq D^2$.) The link variables a_{xy} can be considered as specifying a weighted graph. Since we want the weight a_{xy} to label entanglement in state $|a_{xy}\rangle$, we can require the entanglement entropy between x and y to be an increasing function of a_{xy}. For example, to be specific we can require

$$S_x(a_{xy}) = a_{xy} \log d, \text{ with } a_{xy} = 0, 1, \ldots, D_L - 1, \; d^{D_L - 1} = D \tag{2.3}$$

which means a_{xy} is the number of EPR pairs across the link, each with dimension d. The maximal a_{xy} corresponds to a maximally entangled state.

In addition, each boundary vertex is connected with a EPR pair state $|xX\rangle_B$ which entangles a qudit at vertex x with one at the boundary physical site X. Then for each configuration $a_{xy} = 0, 1, 2, \ldots, D_L - 1$, an RTN is defined by

$$|\Psi[\{a_{xy}\}]\rangle = \prod_x \langle V_x| \prod_{x \neq y} |a_{xy}\rangle \prod_x |xX\rangle_B \tag{2.4}$$

If we only want to incorporate superposition of RTN on different graphs, the simplest choice will be $D_L = 2$, in which case a qubit at each link determines whether the link is

---

[1]Similar link variables have been introduced in perfect tensor networks in ref. [26] for a different but related purpose.

connected (entangled) or not. However, it is more convenient to introduce a larger D_L, which makes it possible to define "small" fluctuations around a classical geometry, as will be discussed in section 4.

The definition (2.4) defines a linear map from the bulk Hilbert space $\mathbb{H}_b$ spanned by the link qubits (with dimension $D_L^{V(V-1)/2}$) to the boundary Hilbert space $\mathbb{H}_B$ (with dimension D^{V_B}), which maps the basis states $\prod_{x\neq y}|a_{xy}\rangle$ to $|\Psi[\{a_{xy}\}]\rangle$. We denote this map by $M : \mathbb{H}_b \rightarrow \mathbb{H}_B$:

$$M\,|\Psi_{\text{bulk}}\rangle \equiv \prod_x \langle V_x|\,|\Psi_{\text{bulk}}\rangle \prod_x |xX\rangle_B \tag{2.5}$$

The Hermitian conjugate operator $M^\dagger : \mathbb{H}_B \rightarrow \mathbb{H}_b$ defines a linear map from the boundary Hilbert space to the bulk Hilbert space. This pair of maps M and $M^\dagger$ can be viewed as a holographic mapping that builds a correspondence between states (on the boundary) and geometries (in the bulk). It is straightforward to generalize the random average technique in ref. [23] to the current setup, which is how we will investigate properties of this holographic mapping in the following sections.

3 Boundary-to-bulk isometry

In this section, we will study the holographic mapping from boundary to bulk, and show that it is an isometry under certain conditions. This result demonstrates that tensor network states $|\Psi[\{a_{xy}\}]\rangle$ for all configurations $\{a_{xy}\}$ forms an overcomplete basis of the boundary Hilbert space, so that any boundary state can be expanded in this basis.

We summarize the result first. The isometry condition requires

$$\rho_B = \sum_{\{a_{xy}\}} |\Psi[\{a_{xy}\}]\rangle\langle\Psi[\{a_{xy}\}]| \propto \mathbb{I} \tag{3.1}$$

Eq. (3.1) is true if the following two conditions are satisfied,

$$(V-1) \gg \frac{2\log D}{\log D_L} \tag{3.2}$$

$$\left|\text{Tr}\left[\rho_{xy}^{\otimes 4} g \otimes h\right]\right|^2 < \text{Tr}\left[\rho_{xy}^{\otimes 4} g \otimes g\right] \text{Tr}\left[\rho_{xy}^{\otimes 4} h \otimes h\right], \ \forall g \neq h \in S_4 \tag{3.3}$$

Eq. (3.2) can be trivially satisfied if $V \gg 1$, while keeping $\log D/\log D_L$ to be $O(1)$. Eq. (3.3) is the property of the density matrix, whose details will be elaborated in the section 3.2 and appendix A.

If we view the tensor network in figure 3 as an entangled state between boundary and bulk link qudits, the isometry condition is equivalent to the statement that the reduced density matrix ρ_B is maximally mixed. To study ρ_B we study its second Renyi entropy

$$e^{-S_B^{(2)}} = \frac{\text{Tr}\left[\rho_B^2\right]}{\text{Tr}\left[\rho_B\right]^2} \tag{3.4}$$

Similar to ref. [23], we study the random average of the numerator and denominator separately, and then study their fluctuations. When the fluctuation is small, we have $\overline{e^{-S_B^{(2)}}} \simeq \overline{\text{Tr}\left[\rho_B^2\right]}/\overline{\text{Tr}\left[\rho_B\right]^2}$.

3.1 The random-averaged isometry condition

A commonly used trick in writing the Renyi entropy is to write

$$\mathrm{Tr}\left[\rho_B^2\right] = \mathrm{Tr}\left[X_B\rho_B \otimes \rho_B\right] = \mathrm{Tr}\left[\left(X_B \otimes I_{\overline{B}}\right)\left(\rho_B \otimes \rho_B\right)\right] \tag{3.5}$$

with $\rho_B = |\Psi\left[\{a_{xy}\}\right]\rangle\langle\Psi\left[\{a_{xy}\}\right]|$ the density matrix of the whole system, and X_B the swap operator acting on two-copies of the system which permutes the two copies in B region. More explicitly, if we denote an orthonormal basis of B region as $|n\rangle_B$, then $X_B |n\rangle_B \otimes |n'\rangle_B = |n'\rangle_B \otimes |n\rangle_B$.

For the state defined in eq. (2.4), ρ_B is

$$\rho_B = \mathrm{tr}_b\left[\left(\prod_x |V_x\rangle\langle V_x|\right)\left(\prod_{x\neq y}\rho_{xy} \otimes \prod_x |xX\rangle_B\langle xX|_B\right)\right] \tag{3.6}$$

$$\text{with } \rho_{xy} = \frac{1}{D_L}\sum_{a=0}^{D_L-1}|a_{xy}\rangle\langle a_{xy}| \tag{3.7}$$

Therefore

$$\overline{\mathrm{Tr}\left[\rho_B^2\right]} = \mathrm{Tr}\left[\left(X_B \otimes \prod_x \overline{|V_x\rangle\langle V_x|^{\otimes 2}}\right)\left(\prod_{x\neq y}\rho_{xy} \otimes \prod_x |xX\rangle_B\langle xX|_B\right)^{\otimes 2}\right]$$

$$= C^{-1}\sum_{R\subseteq\text{bulk}}\mathrm{Tr}\left[X_{B\cup R}\left(\prod_{x\neq y}\rho_{xy} \otimes \prod_x |xX\rangle_B\langle xX|_B\right)^{\otimes 2}\right] \tag{3.8}$$

Here we have used the mathematical fact that the random average $\overline{|V_x\rangle\langle V_x|^{\otimes 2}} \propto \mathbb{I}_x\otimes\mathbb{I}_x + X_x$, with X_x the swap operator defined in the same way as X_B, acting on all qudits at site x. The normalization constant $C = \left(D^{2V-2} + D^{V-1}\right)^{V_b}\left(D^{2V} + D^V\right)^{V_B}$.

The right-hand side of eq. (3.8) is a sum over the purity of the state $\prod_{x\neq y}\rho_{xy} \otimes \prod_x |xX\rangle_B\langle xX|_B$ for different regions $B \cup R$, with R running over all 2^V subsets of the V vertices. Since this state is simple, with only bipartite entanglement between different sites, the purity can be explicitly computed. In the same way as in ref. [23], the sum can be expressed as a partition function of a classical Ising model, with an Ising spin $s_x = \pm 1$ defined on each site. Each spin configuration corresponds to a region $R_\downarrow$ which is defined as the spin $s = -1$ domain. The action of the Ising model $\mathcal{A}\left[\{s_x\}\right]$ is defined such that $e^{-\mathcal{A}[\{s_x\}]} = \mathrm{Tr}\left[X_{B\cup R_\downarrow}\left(\prod_{x\neq y}\rho_{xy} \otimes \prod_x |xX\rangle_B\langle xX|_B\right)^{\otimes 2}\right]$. Since the state on the righthand side only contains bipartite entanglement, the Ising model action only contains one-body and two-body terms:

$$\mathcal{A}\left[\{s_x\}\right] = -\frac{J}{2}\sum_{xy}\left(s_x s_y - 1\right) - \frac{h}{2}\sum_x s_x + \frac{1}{2}\log D\sum_{x\in B}s_x \tag{3.9}$$

$$\text{with } h = \frac{V-1}{2}\log D_L, \quad J = s_b - \frac{1}{2}\log D_L = \frac{1}{2}\left(S_x^{(2)} + S_y^{(2)} - S_{xy}^{(2)}\right)$$
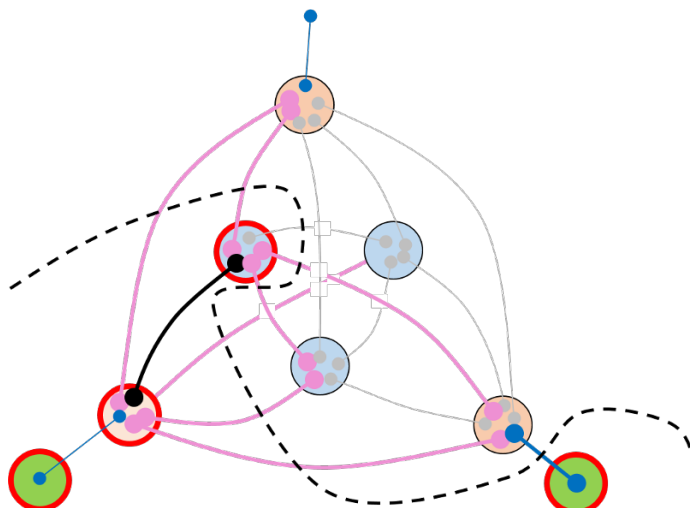
Figure 4. Illustration of a spin configuration with $n_b = n_B = 1$. The spins are -1 for all sites with a thick red circle, and $+1$ elsewhere. The dashed line is the domain wall across which the spin changes sign. The contribution to the action comes from three kinds of links, those within the spin down region (black thick line), those between opposite spins (pink thick line) and those connecting the spin up boundary sites to the boundary (blue thick line). These three contributions correspond to $\mathcal{A}_{1,2,3}$ in eq. (3.10) respectively.

Here $0 < s_b \leq \log D$ is the second Renyi entropy of site x in the state ρ_{xy}, i.e. $e^{-s_b} = \operatorname{tr}_x(\operatorname{tr}_y \rho_{xy})^2$, and the Ising coupling J is half of the second Renyi mutual information between sites x, y in the mixed state ρ_{xy}. The last term in the action sums over the V_B boundary sites.

The Ising model problem is simpler than that for a generic RTN in ref. [23] because all pairs of x, y are coupled equally. Consequently, all V_b bulk vertices are equivalent, and all V_B boundary vertices are equivalent. The action is therefore only a function of two integers, the number of down spins in the bulk vertices $n_b \in [0, V_b]$, and the number of down spins in the boundary vertices $n_B \in [0, V_B]$.

$$\mathcal{A}\left[\{s_x\}\right] = \mathcal{A}(n_b, n_B) = \mathcal{A}_1 + \mathcal{A}_2 + \mathcal{A}_3$$
$$\mathcal{A}_1 = \log D_L (n_b + n_B)(n_b + n_B - 1)/2,$$
$$\mathcal{A}_2 = s_b (n_b + n_B)(V - n_b - n_B), \quad \mathcal{A}_3 = \log D (V_B - n_B) \tag{3.10}$$

The three terms $\mathcal{A}_{1,2,3}$ are contributions of links within region R, links between R and its complement, and links from $\overline{R}$ to the boundary, respectively, as is illustrated in figure 4.

With the action $\mathcal{A}(n_b, n_B)$, eq. (3.8) becomes

$$\overline{\operatorname{Tr}\left[\rho_B^2\right]} = C^{-1} \sum_{n_b=0}^{V_b} \sum_{n_B=0}^{V_B} \binom{V_b}{n_b} \binom{V_B}{n_B} e^{-\mathcal{A}(n_b, n_B)} \tag{3.11}$$

For large V_b, V_B, this sum is dominated by the biggest term, which corresponds to the minimum of $\mathcal{S}(n_b, n_B) = \mathcal{A}(n_b, n_B) - \log\binom{V_b}{n_b} - \log\binom{V_B}{n_B}$. One can show that

$\mathcal{S}\left(n_b, n_B\right)$ reaches its minimum in the large V_b, V_B limit at one of the corners in region $n_b \in [0, V_b]$, $n_B \in [0, V_B]$. A detailed explanation can be found in appendix A.1. The same analysis applies to the denominator $\overline{\mathrm{Tr}\left[\rho_B\right]^2}$, and the only difference is in the boundary term $\mathcal{A}_3$.

$$\overline{\mathrm{Tr}\left[\rho_B\right]^2} = C^{-1} \sum_{n_b=0}^{V_b} \sum_{n_B=0}^{V_B} \binom{V_b}{n_b} \binom{V_B}{n_B} e^{-\tilde{\mathcal{A}}(n_b, n_B)} \tag{3.12}$$

with $\tilde{\mathcal{A}} = \mathcal{A}_1 + \mathcal{A}_2 + \tilde{\mathcal{A}}_3$ and $\tilde{\mathcal{A}}_3 = n_B \log D$.

The isometry condition is satisfied if the dominant configuration for both the numerator and the denominator is given by $n_B = n_b = 0$, which requires

$$\log D_L \frac{V(V-1)}{2} > V_B \log D \tag{3.13}$$

$$\log D_L \frac{V_B(V_B-1)}{2} + s_b V_b V_B > V_B \log D \tag{3.14}$$

Condition (3.13) is simply a requirement that the bulk Hilbert space dimension $D_L^{V(V-1)/2}$ is larger than that of the boundary (D^{V_B}). Condition (3.14) requires that the link state ρ_{xy} is sufficiently entangled. In term of coupling $J = s_b - \frac{1}{2}\log D_L$, the condition (3.14) requires

$$J > \frac{1}{V_b}\left(\log D - \frac{V-1}{2}\log D_L\right) \tag{3.15}$$

Condition (3.13) and (3.14) are easy to satisfy. If we take the limit $V_b, V_B \to \infty$ with the ratio V_B/V fixed, and keep D, D_L to be $O(1)$, all conditions will be trivially satisfied.

The isometry condition (3.1) allows an expansion of an arbitrary boundary state $|\Phi\rangle$ in this basis: $|\Phi\rangle = \sum_{\{a_{xy}\}} |\Psi\left[\{a_{xy}\}\right]\rangle \langle \Psi\left[\{a_{xy}\}\right]| \Phi\rangle = \sum_{\{a_{xy}\}} \phi\left[\{a_{xy}\}\right] |\Psi\left[\{a_{xy}\}\right]\rangle$. This wavefunction is the analog of Wheeler-de Witt wavefunction [27] of quantum gravity, although here we are only taking superpositions of spatial geometries.

3.2 Fluctuations

As we discussed earlier, the calculation of $\overline{\mathrm{Tr}\left[\rho_B^2\right]}$ only tells us the average of second Renyi entropy if the fluctuation is small. The fluctuation can be studied by computing $\overline{\left(\mathrm{Tr}\left[\rho_B^2\right]^2\right)} - \left(\overline{\mathrm{Tr}\left[\rho_B^2\right]}\right)^2$. As has been shown in ref. [23], the random average of a quantity like $\overline{\left(\mathrm{Tr}\left[\rho_B^2\right]^2\right)}$, which is quartic in ρ_B, can be expressed as a partition function of a statistical model with a pseudo-spin g_x at each site taking values in the 4-element permutation group S_4. In general, any quantity in the form of $\mathrm{Tr}\left[\rho^{\otimes k} O_k\right]$, with operator O_k acting on k copies of the system,[2] is mapped to a partition function of a model with pseudo-spins in k-element permutation group S_k. Similar to the Ising model analyzed above, the statistical models for higher k is also defined on a complete graph, which simplifies the problem. In

---

[2]For example, $\mathrm{Tr}\left[\rho_A^k\right]$ which determines the k-th Renyi entropy can be written as $\mathrm{Tr}\left[\rho^{\otimes k} C_{Ak}\right]$ with C_{Ak} the cyclic permutation of the k copies of systems in A region.

appendix A we analyze these pseudospin models and obtain sufficient conditions for fluctuations such as $\overline{\left(\text{Tr}\left[\rho_B^2\right]^2\right)} - \overline{\text{Tr}\left[\rho_B^2\right]}^2$ to be controlled. For bounding the fluctuation of the second Renyi entropy calculation, the sufficient conditions are the following:

$$(V-1) \gg \frac{2\log D}{\log D_L} \tag{3.16}$$

$$\left|\text{Tr}\left[\rho_{xy}^{\otimes k} g \otimes h\right]\right|^2 < \text{Tr}\left[\rho_{xy}^{\otimes k} g \otimes g\right] \text{Tr}\left[\rho_{xy}^{\otimes k} h \otimes h\right], \ \forall g \neq h \in S_k \tag{3.17}$$

with $k = 4$ in the second equation. More details of the derivation will be given in appendix A. It is not difficult to see that conditions (3.16) and (3.17) imply the conditions we obtain earlier in eq. (3.13) (3.15). Condition (3.16) can be easily satisfied in large volume V. Condition (3.17) imposes addition constraints to the choice of states $|a_{xy}\rangle$ and ρ_{xy}, but is also not hard to satisfy, as we will discuss in more details in appendix A. We also give an explicit example of $|a_{xy}\rangle$ in appendix A.3 which satisfies condition (3.17) for general k.

4 Bulk-to-boundary isometry in code subspaces

Since the bulk basis $|\Psi\left[\{a_{xy}\}\right]\rangle$ is generically overcomplete, the mapping from bulk to boundary defined by our random tensor network is not injective. However, holographic duality requires that small fluctuations around a classical geometry are independent physical states on the boundary. For example, if we consider a dilute gas of gravitons in the bulk, the total degree of freedom of the gas is proportional to volume. Gravitons at different bulk locations should be dual to independent degrees of freedom on the boundary, since graviton creation/annhilation operators should be mapped to independent operators on the boundary by the dictionary of holographic duality. This requirement means that there should be a bulk-to-boundary isometry in the subspace of such small fluctuations. The bulk small fluctuations are mapped to a subspace of the boundary Hilbert space, named as the "code subspace"[21, 24]. Each geometry corresponding to a configuration $a = \{a_{xy}\}$ defines a code subspace $\mathbb{H}_C[a]$. The mapping of such small fluctuations to the boundary should satisfy the following local reconstruction property: each region on the boundary A corresponds to a minimal surface γ_A in the bulk that is homologous to it. The region enclosed by $A \cup \gamma_A$ is the entanglement wedge E_A.[3] A bulk operator acting in the subspace of small fluctuations (the *code subspace*) in the bulk region E_A can be reconstructed in boundary region A. Since each bulk point can be enclosed by the entanglement wedges of different boundary regions, information in the bulk can be recovered from different boundary regions, making the bulk-boundary map in the code subspace a quantum error correction code [24]. The bulk-boundary isometry and local reconstruction is illustrated in figure 5.

In the following we will explain how our formalism of fluctuating geometry allows the definition of small fluctuations and code subspaces. In section 4.1, we obtain the condition of code subspaces in which global reconstruction (*i. e.* bulk-to-boundary isometry) can be

---

[3]More precisely, E_A here is the intersection of the entanglement wedge and the spatial slice. Since we will always be dealing with a spatial slice, we neglect this difference and call E_A the entanglement wedge.
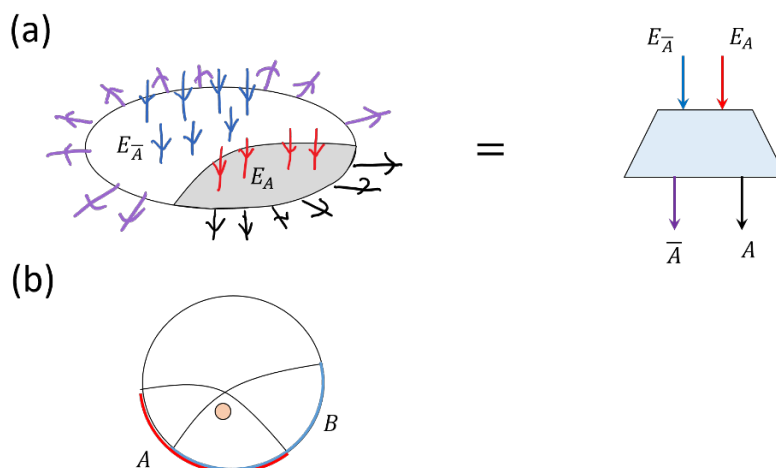
Figure 5. (a) Illustration of the bulk-boundary map defined in the code subspace. The mapping from the whole bulk subspace to the boundary is an isometry. Furthermore, the local reconstruction property requires that degrees of freedom in $E_{\overline{A}}$ which is the entanglement wedge of A can be reconstructed in A, which means an isometry is defined from E_A to A for arbitrary states in $E_{\overline{A}}$ and $\overline{A}$. (b) A small region in the bulk (orange disk) can be reconstructed in different boundary regions such as A, B.

defined. A sufficient condition is given in eq. (4.7) and (4.8). In section 4.2, we discuss the condition of local reconstruction on a subregion of the boundary.

4.1 Classical geometry and the code subspace

Each configuration $\{a_{xy}\}$ corresponds to a "geometry" (i.e. a weighted graph), but if a_{xy} takes arbitrary values, one cannot define what fluctuations are considered "small". With a large link variable dimension D_L, one can define a classical geometry as one with all non-trivial links ($a_{xy} \neq 0$) contributing a large entropy $\propto D_L$, and then define small fluctuations as fluctuations of a_{xy} that are small compared to D_L.

For concreteness, we pick a value of link variable a_0 with $0 < \frac{a_0}{D_L-1} < 1$, and take the limit $D_L, D \to \infty$ with $\frac{a_0}{D_L-1}$ fixed. We define a classical geometry by a state $|\Psi[\{a_{xy}\}]\rangle$ with all a_{xy} equal to either a_0 or 0.[4] For such states, we can define an adjacent matrix K with $K_{xy} = 0, 1$, such that $a_{xy} = K_{xy}a_0$.

Now define a range of small fluctuation $\Lambda \ll a_0$. In the limit $D_L \to \infty$, Λ is kept finite. Then we define small fluctuations around the classical geometry $K_{xy}a_0$ as all states $|\Psi[\{a_{xy}\}]\rangle$ satisfying

$$
\begin{cases}
a_{xy} \in [a_0 - \Lambda, a_0 + \Lambda], & \text{if } K_{xy} = 1 \\
a_{xy} \in [0, 2\Lambda], & \text{if } K_{xy} = 0
\end{cases}
\tag{4.1}
$$

---

[4]It is straightforward to generalize the following discussion to states with different a_0 on different links as long as all of them are taken to infinity with the ratio $a_0/(D_L - 1)$ fixed.
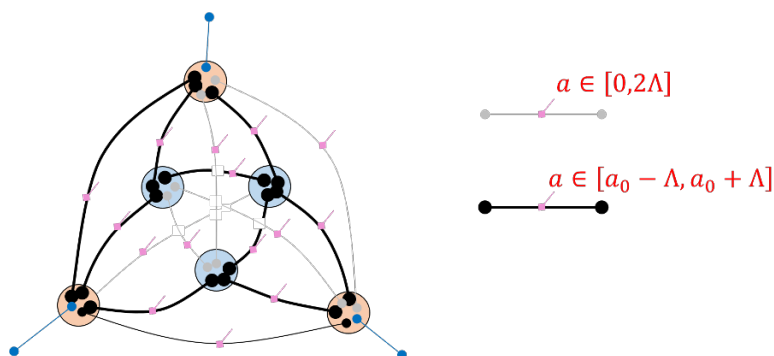
Figure 6. Illustration of small fluctuations around a classical geometry. In the classical geometry, the black thick lines and grey thin lines are connected links with $a_{xy} = a_0$ and disconnected links with $a_{xy} = 0$, respectively. The fluctuations are encoded by fluctuation of link quantum number a around the classical value in a small range.

This range of a_{xy} defines a subspace of the bulk, which is mapped to the boundary by the random tensor network. The definition of the classical geometry and small fluctuation subspace is illustrated in figure 6.

To study whether the bulk-boundary map is an isometry, we carry the same calculation as in section 3 to evaluate the second Renyi entanglement entropy between bulk and boundary. An isometry is defined if the bulk subspace is maximally entangled with the boundary. The calculation is exactly parallel to that in section 3, except that the bulk link state ρ_{xy} in eq. (3.6) is replaced by

$$\rho_{xy} = \begin{cases} \rho_1 = \dfrac{1}{2\Lambda + 1} \displaystyle\sum_{\delta a_{xy}=-\Lambda}^{\Lambda} |a_0 + \delta a_{xy}\rangle \langle a_0 + \delta a_{xy}|, & \text{if } K_{xy} = 1 \\[4mm] \rho_2 = \dfrac{1}{2\Lambda + 1} \displaystyle\sum_{\delta a_{xy}=0}^{2\Lambda} |\delta a_{xy}\rangle \langle \delta a_{xy}|, & \text{if } K_{xy} = 0 \end{cases} \tag{4.2}$$

The Ising action is changed correspondingly to

$$\mathcal{A}\left[\{s_x\}\right] = \mathcal{A}_0\left[\{s_x\}\right] + \delta\mathcal{A}\left[\{s_x\}\right]$$
$$\mathcal{A}_0\left[\{s_x\}\right] = -\frac{J_1}{2}\sum_{\langle xy\rangle \in K}(s_x s_y - 1) + \frac{1}{2}\log D \sum_{x\in B} s_x$$
$$\delta\mathcal{A}\left[\{s_x\}\right] = -\frac{J_2}{2}\sum_{\langle xy\rangle \neq K}(s_x s_y - 1) - \frac{h_C}{2}\sum_{x} s_x \tag{4.3}$$
$$\text{with } h_C = \frac{V-1}{2}\log\left(2\Lambda + 1\right),$$
$$J_1 = s_b\left[\rho_1\right] - \frac{1}{2}\log\left(2\Lambda + 1\right), \ \ J_2 = s_b\left[\rho_2\right] - \frac{1}{2}\log\left(2\Lambda + 1\right)$$

Here $J_{1,2}$ are half the Renyi mutual information of the states $\rho_{1,2}$ on the connected and the disconnected links respectively.

In the limit of $J_1 \gg J_2$, $\log D \to \infty$ with h_C and Λ finite, $\mathcal{A}_0$ is the leading term in the action, and $\delta\mathcal{A}$ is a subleading correction.

The analysis of this action is essentially the same as the original RTN case in ref. [23]. The boundary term prefers $s_x = -1$, while the bulk pinning field h_C prefers $s_x = +1$. Isometry condition is satisfied in the limit $\log D \to \infty$, $J_1 \to \infty$ if the lowest action configuration is $s_x = -1$ everywhere, which corresponds to an entropy $h_C V = \frac{V(V-1)}{2} \log(2\Lambda + 1) = \log(\dim \mathbb{H}_C)$. In order for this configuration to have the lowest action, one requires that creating any spin up domain R costs a positive action. Denoting the action of a spin configuration with $s_x = +1$ in R and $s_x = -1$ elsewhere as $\mathcal{A}_R$, the isometry requirement is

$$\mathcal{A}_R - \mathcal{A}_\emptyset = (J_1 - J_2)\,|\partial R| + J_2\,|R|\,(V - |R|)$$
$$+ \log D\,|R \cap B| - h_C |R| > 0,\ \forall R \subseteq \text{bulk} \tag{4.4}$$

where the first two terms are action cost from the two-body interaction terms, the third term is the action cost from boundary pinning fields, while the last term is the action saved by the external field term h_C. $|R|$ is the number of vertices in R and $|\partial R|$ is the number of links connecting R and its complement in graph K (excluding the boundary links). $|\partial R \cap B|$ is the number of links connecting R with boundary, i.e. the number of boundary sites in R.

For sufficiently large J_1, $\log D$ and finite J_2, h_C, condition (4.4) is satisfied. To obtain a more explicit understanding on the requirements, in the following we derive a sufficient condition which guarantees that the isometry condition (4.4) is satisfied for *all* classical geometries. Denote N and M as the number of interior sites and boundary sites in R, respectively, such that $|R| = N + M$ and $|R \cap B| = M$. The action cost $\Delta\mathcal{A} \equiv \mathcal{A}_R - \mathcal{A}_\emptyset$ is a function of N, M and the graph dependent parameter $|\partial R|$. If we are considering a particular given graph, $|\partial R|$ is not independent from N and M. However, simplification occurs when we require condition (4.4) to hold for all R and for *all* classical geometries. By varying the graph, one can always vary $|\partial R|$ of a given region R in the range $\left[0, \frac{(N+M)(V-N-M)}{2}\right]$). Therefore we can view the action cost $\Delta\mathcal{A}$ as a function of three independent variables $N, M, |\partial R|$. This simplified the problem of minimizing $\Delta\mathcal{A}$, because the function in eq. (4.4) does not have local minimum in term of N, M and $|\partial R|$. Thus the minimum can only occur at corners of the parameter space. Given that $J_1 - J_2 > 0$, the minimum always occurs at $|\partial R| = 0$, in which case $\Delta\mathcal{A} = J_2 (N + M)(V - N - M) + M \log D - h_C(N + M)$. Evaluating $\Delta\mathcal{A}$ at the four corners $N = 0$ or V_b and $M = 0$ or V_B leads to two nontrivial conditions:

$$\Delta\mathcal{A}(V_b, V_B) > 0 \Rightarrow V_B \log D > \frac{V(V-1)}{2} \log(2\Lambda + 1) \tag{4.5}$$

$$\Delta\mathcal{A}(V_b, 0) > 0 \Rightarrow J_2 V_b V_B > \frac{V_b(V-1)}{2} \log(2\Lambda + 1) \tag{4.6}$$

In summary the two sufficient conditions are

$$\log D > \frac{V(V-1)}{2V_B} \log(2\Lambda + 1) \tag{4.7}$$

$$J_2 > \frac{(V-1)}{2V_B} \log(2\Lambda + 1) \tag{4.8}$$

Physically, the first condition (4.7) is simply the requirement that the bulk code subspace has smaller dimension than the boundary. The second condition requires that even weak links with coupling J_2 provide strong enough entanglement to propagate information from bulk to boundary isometrically. It should be noted that condition (4.7) requires D to grow exponentially with volume V (if we fix the ratio V_B/V). This is necessary since the bulk code subspace dimension grows with $(2\Lambda + 1)^{V(V-1)/2}$. Besides, eq. (4.8) only requires J_2 to be a $O(1)$ number in this limit. If we consider a limit $V \to \infty$ with large but finite D, it will be impossible to faithfully represent all link variable fluctuations δa_{xy} to the boundary. However, it is probably still possible to define a code subspace with lower bound dimension, which contains bulk excitations with a low enough density. (An example of such kind of code subspace was discussed in ref. [22].) Such a code subspace which is not a direct product of Hilbert spaces of each link is probably closer to the code subspace in AdS/CFT, consisting low energy bulk quantum field theory excitations.

4.2 Local reconstruction properties

Now we further investigate the local reconstruction properties of the bulk-boundary isometry. The local reconstruction requirement can be phrased in an entanglement entropy calculation. In the old setup of tensor networks with fixed geometry, shown in figure 5, one can view the bulk-boundary map as a quantum state that contains four partitions $A, \overline{A}, E_A, E_{\overline{A}}$. The requirement that A contains all information about E_A is equivalent to the statement $I(E_A : \overline{A}) = S(E_A) + S(\overline{A}) - S(E_A\overline{A}) = 0$. In the following we will evaluate the second Renyi entropy version of the mutual information. In the large D limit when the fluctuation of Renyi entropies are small, we expect the von Neumann entropy to be equal to the Renyi entropy. Before proceeding, we would like to note that in the current setup the bulk degrees of freedom are defined on links, so that the bulk Hilbert space do not factorize into different regions. For a boundary region A, one can define an entanglement wedge E_A, such that all links with both ends contained in E_A can be reconstructed from A. In the following we will demonstrate that under certain conditions, the region enclosed by a boundary region A and the minimal surface γ_A homologous to A is the entanglement wedge E_A. This is illustrated in figure 7.

Since we need to compute Renyi entropy of regions including both bulk and boundary, we should not trace over bulk link variables to obtain a reduced density matrix ρ_{xy}. Instead we treat the whole RTN with bulk and boundary indices as a state, and map the second Renyi entropy calculation to an Ising model partition function. All dangling ends of the tensor network in bulk and boundary correspond to fixed external spins that couple to the dynamical Ising spins defined on bulk vertices. We denote the dynamical Ising spins as s_x, and the external spins as m_X on the boundary and m_{xy} on bulk links. s_x, m_X, m_{xy} all take values of ± 1. When we compute the Renyi entropy of a bulk region E_A and a boundary region $\overline{A}$, the external spins are defined as

$$m_X = \begin{cases} -1, & X \in \overline{A} \\ +1, & X \notin \overline{A} \end{cases}, \qquad m_{xy} = \begin{cases} -1, & xy \in E_A \\ +1, & xy \notin E_A \end{cases} \tag{4.9}$$
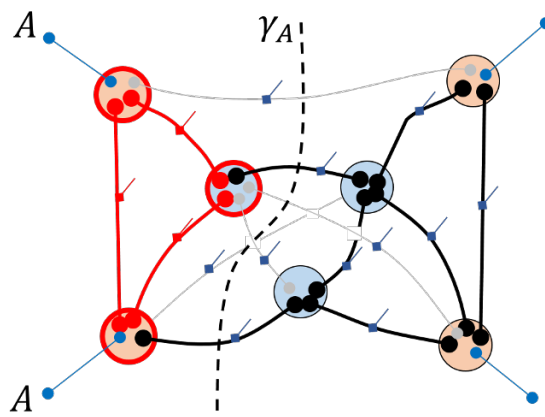
Figure 7. Illustration of the entanglement wedge of a boundary region A. The vertices with red circles are the entanglement wedge E_A, enclosed by A and the minimal surface γ_A. The code subspace that can be locally reconstructed in region A are labeled by links with both ends in E_A, marked by red bulk lines. (For clarity we have only drawn a few of the unconnected (grey) links.)

For small fluctuations around a graph K considered here, we have

$$\overline{\mathrm{Tr}\left[\rho^2_{A\cup b}\right]} = \mathrm{const.} \sum_{\{s_x=\pm1\}} e^{-\mathcal{A}[\{s_x\}]}$$

$$\mathcal{A}\left[\{s_x\}\right] = -\frac{J_1}{2} \sum_{\langle xy\rangle \in K} (s_x s_y - 1) - \frac{J_2}{2} \sum_{\langle xy\rangle \notin K} (s_x s_y - 1)$$
$$-\frac{1}{2}\log D \sum_{x\in B} s_x m_X - \frac{1}{4}\log(2\Lambda+1)\sum_{xy} m_{xy}(s_x+s_y) \qquad (4.10)$$

J_1 and J_2 are the same as in eq. (4.3). The earlier calculation of the entropy of entire boundary in eq. (4.3) corresponds to the special case $m_{xy} = +1$, $\forall x,y$ and $m_X = -1$, $\forall X$. The constant prefactor is not important as it is the same for all configurations, and does not affect normalized quantities such as $\overline{\mathrm{Tr}\left[\rho^2_{A\cup b}\right]}/\overline{\mathrm{Tr}\left[\rho_{A\cup b}\right]}^2$. Similarly, $\overline{\mathrm{Tr}\left[\rho_A\right]}^2$ and $\overline{\mathrm{Tr}\left[\rho_b\right]}^2$ can be computed by the same action with different boundary conditions.

The mutual information is determined by the correlation between external spins mediated by the dynamical spins. We denote the effective action $\mathcal{A}_{\mathrm{eff}}^{--} = -\log\overline{\mathrm{Tr}\left[\rho^2_{\bar{A}\cup E_A}\right]}$ as the effective action with boundary condition (4.9), with $--$ labeling the sign of external spin in $\bar{A}$ and E_A respectively. Similarly $\mathcal{A}_{\mathrm{eff}}^{-+} = -\log\overline{\mathrm{Tr}\left[\rho^2_{\bar{A}}\right]}$, $\mathcal{A}_{\mathrm{eff}}^{+-} = -\log\overline{\mathrm{Tr}\left[\rho^2_{E_A}\right]}$, and $\mathcal{A}_{\mathrm{eff}}^{++} = \overline{\mathrm{Tr}\left[\rho\right]}^2$ is the normalization constant. Then

$$I^{(2)}(E_A : \overline{A}) = S_{\bar{A}}^{(2)} + S_{E_A}^{(2)} - S_{\bar{A}E_A}^{(2)} \simeq \mathcal{A}_{\mathrm{eff}}^{+-} + \mathcal{A}_{\mathrm{eff}}^{-+} - \mathcal{A}_{\mathrm{eff}}^{++} - \mathcal{A}_{\mathrm{eff}}^{--} \qquad (4.11)$$

is determined by the "energy cost" of the external spins in $\bar{A}$ and E_A being anti-parallel. The requirement of zero mutual information is equivalent to the requirement that the two external spins are completely uncorrelated. It is easy to see that this is true in the limit we consider, with $J_1, \log D \to \infty$ and J_2, Λ finite. In this limit, the spin configuration

s_x is completely determined by boundary external spins m_X, and thus $I^{(2)}(E_A : \overline{A}) = 0$. For finite $J_1, \log D$, the local reconstruction condition depends on more detailed properties of the classical geometry. Although it is possible to write down some sufficient condition by taking J_1 and $\log D$ to be very large, we feel these conditions are not so useful to include here.

5 Overlap between different classical geometries

In the discussion above we have shown that each classical geometry labeled by a graph K is accompanied with a code subspace that satisfies bulk-boundary isometry and local reconstruction properties. The next question is whether the code subspaces for different classical geometries are truely independent subspaces of the boundary Hilbert space. Since the basis $|\Psi\left[\{a_{xy}\}\right]\rangle$ is over-complete, different geometries are generically not orthogonal, but in the following we will show that states in the code subspace of different classical geometries have exponentially small overlap.

For this purpose we study the overlap $C_{ab} = \langle\Psi\left[\{a_{xy}\}\right]|\Psi\left[\{b_{xy}\}\right]\rangle$ between two generic geometries a_{xy} and b_{xy}. Using the definition (2.4) we have

$$C_{ab} = D^{-V_B}\text{Tr}\left[\prod_x |V_x\rangle\langle V_x|\prod_{x\neq y}|b_{xy}\rangle\langle a_{xy}|\right] \tag{5.1}$$

Carrying the random average one obtains

$$\overline{C_{ab}} = D^{-(V-1)V_b - VV_B}\delta_{ab} \tag{5.2}$$

It is essential to go to the second order and study the fluctuation around the average value, so that we evaluate $\overline{|C_{ab}|^2}$:

$$\overline{|C_{ab}|^2} = D^{-2V_B}\text{Tr}\left[\prod_x \overline{|V_x\rangle\langle V_x|^{\otimes 2}}\left(\prod_{x\neq y}|b_{xy}\rangle\langle a_{xy}|\otimes|a_{xy}\rangle\langle b_{xy}|\right)\right]$$

$$= D^{-2V_B}\Omega^{-1}\sum_{R\subseteq\text{bulk}}\text{Tr}\left[X_R\prod_{x\neq y}|b_{xy}\rangle\langle a_{xy}|\otimes|a_{xy}\rangle\langle b_{xy}|\right]$$

$$= \Omega^{-1}\sum_{R\subseteq\text{bulk}}\text{Tr}\left[X_R\prod_{x\neq y}|b_{xy}\rangle\langle a_{xy}|\otimes|a_{xy}\rangle\langle b_{xy}|\right]D^{-|R\cap B|} \tag{5.3}$$

with $\Omega = \left(D^{V-1} + D^{2(V-1)}\right)^{V_b}\left(D^V + D^{2V}\right)^{V_B}$. To simplify this expression we can write $X_R = X_{\overline{R}}X_{\text{tot}}$ with X_{tot} the swap of all bulk vertices. X_{tot} will simply permute $|b_{xy}\rangle$ and $|a_{xy}\rangle$. Relabel $\overline{R}$ by R we obtain

$$\overline{|C_{ab}|^2} = \Omega^{-1}\sum_{R\subseteq\text{bulk}}\text{Tr}\left[X_R\prod_{x\neq y}|a_{xy}\rangle\langle a_{xy}|\otimes|b_{xy}\rangle\langle b_{xy}|\right]D^{|R\cap B|-V_B}$$

$$= \Omega^{-1}\sum_{R\subseteq\text{bulk}}\text{Tr}\left[\rho_R^a\rho_R^b\right]D^{|R\cap B|-V_B} \tag{5.4}$$

Here ρ_R^a is the reduced density matrix of $\prod_{xy} |a_{xy}\rangle \langle a_{xy}|$ in region R, and similarly for ρ_R^b. If we consider the term with R the entire bulk, $\mathrm{Tr}\left[\rho_R^a \rho_R^b\right] = |\langle a|b\rangle|^2 = \delta_{ab}$ is the inner-project of the two bulk states. Roughly speaking, we can consider all other terms as corrections to the overlap induced by the bulk-boundary map that is not injective.

The overlap $\mathrm{Tr}\left[\rho_R^a \rho_R^b\right]$ is nonzero only if $a_{xy} = b_{xy}$ for all $x, y \in R$. Denote the set of R that satisfy this property as $\mathcal{C}$. To obtain an upper bound of the overlap, we use the inequality

$$\mathrm{Tr}\left[\rho_R^a \rho_R^b\right] \leq \sqrt{\mathrm{Tr}\left[\rho_R^a\right]^2 \mathrm{Tr}\left[\rho_R^b\right]^2} = e^{-\frac{1}{2}\left(S_a^{(2)}(R) + S_b^{(2)}(R)\right)} \tag{5.5}$$

where $S_{a,b}^{(2)}(R)$ are the second Renyi entropy of states $|a_{xy}\rangle$ and $|b_{xy}\rangle$ in region R. Therefore

$$\overline{|C_{ab}|^2} \leq \Omega^{-1} \sum_{R \in \mathcal{C}} e^{-\frac{1}{2}\left(S_a^{(2)}(R) + S_b^{(2)}(R)\right) - \log D(V_B - |R \cap B|)} \tag{5.6}$$

To understand the physical meaning of eq. (5.6), we evaluate it in several situations.

1. *The diagonal element.* If $a_{xy} = b_{xy} \ \forall x, y$, R can be any subset of the bulk, and the dominant term in the sum is given by $R =$ entire bulk. Also in this case, the inequality takes the equal sign. If we take the classical geometry discussed in this section, with $J_1, \log D \to \infty$, we can ignore the contribution of other terms, and obtain $\overline{C_{aa}^2} \simeq \Omega^{-1}$. Therefore

$$\frac{\overline{C_{aa}^2}}{\overline{C_{aa}}^2} \simeq \left(1 + D^{1-V}\right)^{-V_b} \left(1 + D^{-V}\right)^{-V_B} \simeq e^{-V_b D^{1-V} - V_B D^{-V}} \tag{5.7}$$

The ratio is close to 1 in the limit of large volume since $V_b D^{1-V}$ and $V_B D^{-V}$ are much smaller than 1. In other words, the fluctuation of the norm of state $|\Psi\left[\{a_{xy}\}\right]\rangle$ is exponentially suppressed, which justifies the computation of $\overline{|C_{ab}|^2}$ without first normalizing the two states.

2. *Completely distinct states.* If we consider two completely distinct states such that $a_{xy} \neq b_{xy} \ \forall x, y$, then the only contribution comes from $R = \emptyset$, and $\overline{|C_{ab}|^2} = \Omega^{-1} D^{-V_B} = \sqrt{\overline{C_{aa}^2 C_{bb}^2}} D^{-V_B}$. In other words, the overlap between these states, after normalization, is the inverse of boundary Hilbert space dimension D^{V_B}. This is equal to the average overlap between two completely random states in the boundary Hilbert space dimension.[5]

3. *Two states different in IR.* Now we study a nontrivial example. In holography all geometries considered are asymptotically anti-de Sitter space in UV (the region near

---

[5]Apparently, when the bulk volume V is large enough so that the basis $|\Psi\left[a_{xy}\right]\rangle$ is very overcomplete, some of them will have a significant overlap. This fact, however, does not appear in the calculation of averaged overlap $\overline{|C_{ab}|^2}$. The higher moments $|C_{ab}|^{2k}$ shall be able to reveal the effect of extremely large V, which we postpone to future works. We would like to thank Lenny Susskind for helpful discussion on this problem.
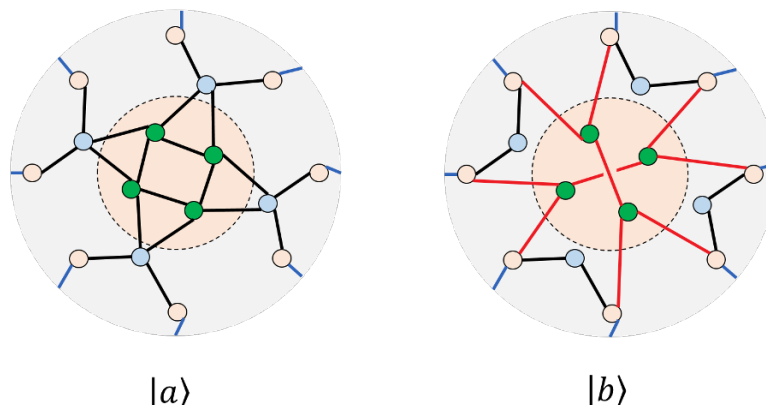
Figure 8. Two graphs with identical edges in the UV region (grey) and different edges in IR (orange) and between the two regions. The overlap of these two states are upper bounded by eq. (5.6), with $|\partial R|_a = |\partial R|_b = 8$.

the boundary) and are generically different in IR. For example we may consider two geometries, one with a black hole in IR and one without black hole. As a toy model of this situation, we can consider two geometries that are identical in a UV region R_m bounding the boundary, and distinct in the IR region, as is illustrated in figure 8. We assume a_{xy} and b_{xy} are completely distinct if x or y are outside region R_m, so that all regions contributing to the overlap are R_m or its subsets. In this case the dominant contribution to eq. (5.6) is given by the $R \subseteq R_m$ that has minimal averaged entropy $\frac{1}{2}\left(S_a^{(2)}(R) + S_b^{(2)}(R)\right)$. If both geometries are classical geometries with all connected links $a_{xy} = a_0$, the entropies satisfy area law $S_{a,b}^{(2)}(R) = s_0 |\partial R|_{a,b}$ with s_0 the entropy contributed by each link state $|a_0\rangle$. $|\partial R|_{a,b}$ denotes the area (number of links crossing the boundary of R) in graphs of a, b respectively. In summary we obtain for two classical geometries a, b

$$\frac{\overline{|C_{ab}|^2}}{\sqrt{\overline{C_{aa}}^2 \overline{C_{bb}}^2}} \leq e^{-\frac{s_0}{2}\left(|\partial R|_a + |\partial R|_b\right)} \tag{5.8}$$

where R is chosen to minimize the averaged area. For example if we consider two geometries with and without a black hole, and assume that the geometry to be identical in UV until a certain distance to the horizon, then $|\partial R|_{a,b} > A_{BH}$ is bounded by the area of black hole horizon, so that the overlap is upper bounded by $e^{-S_{BH}}$. More generally, the overlap is bounded by the entropy of the minimal area surface that enclose the region where the two geometries are (macroscopically) distinct.

From our definition of code subspace, it's clear that if two classical geometries are distinct at a link xy, the small fluctuations $a_{xy} + \delta a_{xy}$ are still distinct from $b_{xy} + \delta b_{xy}$. Therefore the overlap upper bound for $\overline{|C_{ab}|^2}$ between two classical geometries a, b also applies to any pair of states from the code subspaces of a and b. Consequently, if we choose a set of macroscopically distinct geometries a_{xy}^n, the code subspaces $\mathbb{H}_{Cn}$ of each of them are

almost orthogonal subspaces of the boundary Hilbert space. One can define a bigger code subspace $\mathbb{H}_C = \oplus_n \mathbb{H}_{Cn}$ such that the bulk-boundary isometry is still well-defined in the bigger code subspace. In the bigger code subspace $\mathbb{H}_C$, operators that can be reconstructed on a boundary region A form an algebra with nontrivial center, a structure that has been investigated in ref. [28]. More specifically, for example one can define an area operator $\mathcal{L}_A = \oplus s_n \mathbb{I}_n$ which takes eigenvalue s_n in each code subspace $\mathbb{H}_{Cn}$. s_n is the number of connected links between E_A and its complement. Similar structure has been explicitly constructed in the perfect tensor networks [21] by introducing link degrees of freedom [26].

We would like to comment a bit more on the mapping between bulk and boundary operators. A generic bulk operator in this code subspace has the form $\phi = \sum_n P_n \phi_n P_n$, with P_n the projection operator onto n-th code subspace $\mathbb{H}_{Cn}$, and ϕ_n an operator acting only in that subspace. If we denote the linera map from boundary to bulk as M, a local operator ϕ_n in the code subspace of geometry a_{xy}^n is mapped to a boundary operator $M^\dagger P_n \phi_n P_n M$. Although the bulk-boundary mapping is linear and isometric, one can consider $P_n M$ as the linear map restricted to a code subspace, which is "state-dependent"[29]. Locality in the bulk can only be defined in a code subspace around a given classical geometry, and the local operators in a code subspace (such as an operator ϕ_{xy} that only slightly changes a_{xy} value for one link) is actually an operator $P_n \phi_{xy} P_n$ in the large bulk Hilbert space. The "state dependence" of operator correspondence in each code subspace is encoded in the support of the operator in the bulk Hilbert space, specified by P_n.

6 Conclusion and discussions

In conclusion, we have shown that the random tensor network states on all graphs form an overcomplete basis of the boundary Hilbert space, which we name as holographic coherent states. A generic boundary state is mapped to a superposition of geometries. The semi-classical geometries are defined as small fluctuations around reference classical geometries with strongly entangled edges. We show that small fluctuations around a classical geometry form a code subspace, the states in which are mapped to the boundary isometrically, with local reconstruction properties. Furthermore, we show that states in the code subspaces of two different classical geometries are almost orthgonal to each other, with their overlap decaying exponentially as a function of the minimal area surface that covers the bulk region in which the two bulk geometries are distinct.

The holographic coherent state basis has a lot of similarity to the coherent state basis of a boson field. If we consider a complex boson field described by a $|\phi|^4$ theory, the coherent state basis $|\phi(x)\rangle$ is an overcomplete basis of the system, with which one can write a path integral representation of the partition function. The action of the system may have multiple local minima, for example configurations with and without vortices. Around each local minimum one can expand the action in small fluctuations, $\mathcal{A}[\phi_c + \delta\phi] \simeq \mathcal{A}_c + \frac{1}{2}\frac{\delta^2 \mathcal{A}}{\delta\phi\delta\phi}\delta\phi\delta\phi$. The quantization of such fluctuations are low energy quasiparticles such as superfluid phonons. The Hilbert space of such quasiparticle excitations is a "low energy subspace" of the entire Hilbert space. Different classical minima $|\phi_{c1}(x)\rangle$, $|\phi_{c2}(x)\rangle$ are not exactly orthogonal, but the overlap of macroscopically different states are exponentially

suppressed. Therefore one can view the low energy excitations associated with each of them as physically independent subspaces.[6] There are two key differences between the holographic coherent states we consider and the boson coherent states. Firstly, the overlap in the former case is suppressed by exponential of the minimal area covering the distinct region, while that in the latter case is suppressed by exponential of the volume of the distinct region, which can be viewed as a manifestation of holographic principle. Secondly, in the gravity case, locality in the bulk is only defined in the code subspaces, which can be seen in the fact that the log of Hilbert space dimension $\log(\dim(\mathbb{H}_C))$ is proportional to the volume of the bulk, while that of the total Hilbert space $\log(\dim(\mathbb{H}))$ is proportional to the boundary. On comparison, in ordinary boson coherent state case both quantities are proportional to the volume of the system.

There are a lot of open questions along this direction. For a given boundary Hamiltonian, a natural problem is to use the holographic coherent states as variational wavefunctions. The geometry described by a_{xy} can be used as a "mean-field order parameter" that is optimized by minimizing the energy. The difficulty of this approach is the random average, which introduces the ambiguity of a local unitary transformation and therefore mixes states with very different energy. In principle, this problem can be solved in the following procedure. For each given geometrical state $|a\rangle \equiv |\Psi\left[\{a_{xy}\}\right]\rangle$, one can consider all local unitary transformations $\prod_{X \in B}^{\otimes} u_X |a\rangle$, with $u_X \in SU(D)$, and variationally determine u_X by minimizing energy. Denote the minimal energy in this class of states as $E[a]$, we can then minimize energy to determine the optimal bulk geometry a_{xy}. It is not clear whether such a variational procedure is technically feasible. We will reserve that to future works.

Another natural question is how to obtain the bulk equation of motion — the analog of Einstein's equation. By writing the boundary dynamics into a path integral in the geometrical basis, one can in principle obtain a bulk action. Is the Einstein equation or its analog the saddle point equation if the bulk action? Will such saddle point equation be related to previous entanglement approaches to Einstein equation [31–36]. Yet another interesting question is whether a similar area-law bound of state inner product exists in general relativity, where the inner product between two states is defined by a path integral with these states as boundary conditions [37, 38]. It is interesting to compare our results with other recent discussions about the overcompleteness of the geometry basis. [39–41]

Acknowledgments

---

[6]It is interesting to note that the ϕ^4 theory example appeared in a related discussion in ref. [30] about state-dependent operators (see section 5).

A Fluctuations and higher Renyi entropies

In section 3, we make the following approximation in the calculation of the second Renyi entropy.

$$\overline{e^{-S_B^{(2)}}} = \overline{\left(\frac{\text{Tr}[\rho_B^2]}{\text{Tr}[\rho_B]^2}\right)} \approx \frac{e^{-A_{\min}^{(2)}[h_1]}}{e^{-A_{\min}^{(2)}[h_0]}} \tag{A.1}$$

where h_1, h_0 denote the boundary field configuration for the calculation of $\text{Tr}[\rho_B^2]$, $\text{Tr}[\rho_B]^2$. This calculation is valid if the fluctuation around the minimum is small [23]. Formally, the following conditions should be satisfied $\overline{\left(\frac{\text{Tr}[\rho_B^2]}{e^{-A_{\min}^{(2)}[h_1]}} - 1\right)^2} \ll 1$, which can be achieved by requiring

$$\overline{\left(\frac{\text{Tr}[\rho_B^2]}{e^{-A_{\min}^{(2)}[h_1]}} - 1\right)^2} \le \frac{\overline{\text{Tr}[\rho_B^2]^2}}{e^{-A_{\min}^{(4)}[h_1]}} - 1 \ll 1 \tag{A.2}$$

Here we have used that $\overline{\text{Tr}[\rho_B^2]} \ge e^{-A_{\min}^{(2)}[h_1]}$, since at finite temperature the partition function receives contributions from all spin configurations, not just the minimal energy configuration. Similarly for the calculation of $\text{Tr}[\rho_B]^2$ one can require $\frac{\overline{\text{Tr}[\rho_B]^4}}{e^{-A_{\min}^{(4)}[h_0]}} - 1 \ll 1$. Thus the calculation of the fluctuation requires the random average over four copies of the density matrix. Similarly, when calculating the kth Renyi entropy, we need to calculate $\text{Tr}[\rho_B^k]$ which involves k copies of the density matrix. For example $\overline{\text{Tr}[\rho_B^4]}$ and $\overline{\text{Tr}[\rho_B^2]^2}$ are both average of 4 copies of density matrices, with different boundary conditions which specify the contraction of indices. More explicitly they can be written as $\overline{\text{Tr}[\rho_B^4]} = \overline{\text{Tr}[\rho^{\otimes 4} h_{(1234)}^B]}$ and $\overline{\text{Tr}[\rho_B^2]^2} = \overline{\text{Tr}[\rho^{\otimes 4} h_{(12)(34)}^B]}$ with $h_{(1234)}^B$ the cyclic permutation acting on 4-copies of B, and $h_{(12)(34)}^B$ the permutation of 12 and 34 acting on the same region.

Therefore in general we can evaluate the random average of k copies of density matrix with an arbitrary boundary condition, and study how to control its deviation from the contribution of the dominant configuration. The k copy quantity with most general boundary condition can be expressed as

$$\overline{Z^{(k)}} \equiv \text{Tr}\left[\overline{\rho^{\otimes k} \prod_{X \in B} h_X}\right]$$
$$= \sum_{g_x^i \in S_k} \prod_{xy} \text{Tr}\left[\rho_{xy}^{\otimes k} g_x^i g_y^j\right] \prod_{x \in B} \text{Tr}\left[\rho_{EPR}^{\otimes k} g_x^i h_X\right] \tag{A.3}$$

with boundary permutations $h_X \in S_k$ defining the boundary conditions. We label the permutation group elements as g_x^i, $i = 0, 1, 2, \ldots, k!-1$, with $g_x^0 = I_x$ the identity operator. The averaged entanglement quantity is mapped to a partition function of a S_k statistical mechanical model defined on the complete graph.

In the following we will prove that the fluctuation of such quantities with general boundary conditions is bounded if the following sufficient conditions are satisfied:

$$(V - 1) \log D_L \gg 2 \log D \tag{A.4}$$
$$\text{Tr}(\rho_{xy}^{\otimes k} g_x^i g_y^i) \text{Tr}(\rho_{xy}^{\otimes k} g_x^j g_y^j) > |\text{Tr}(\rho_{xy}^{\otimes k} g_x^i g_y^j)|^2, \quad \forall, i \ne j \tag{A.5}$$

In section A.1, we bound the fluctuations based on conditions (A.4) and eq. (A.5). In section A.2, we propose a stronger condition of the density matrix that implies eq. (A.5). In section A.3, we construct the an explicit example in spin system and show that eq. (A.4) and eq. (A.5) are satisfied.

A.1 General results

In this section, we prove that eq. (A.4) and eq. (A.5) are sufficient to bound the fluctuations and to guarantee that higher Renyi entropies are close to the maximum.

First we rewrite eq. (A.5) as

$$L^{ii}(k) + L^{jj}(k) - 2L^{ij}(k) > 0 \tag{A.6}$$

where

$$L^{ij}(k) = -\frac{1}{2}\left(\log \operatorname{Tr}(\rho_{xy}^{\otimes k} g_x^i I_y) + \log \operatorname{Tr}(\rho_{xy}^{\otimes k} I_x g_y^j) - \log \operatorname{Tr}(\rho_{xy}^{\otimes k} g_x^i g_y^j)\right) \tag{A.7}$$

Next, it is straightforward to show that eq. (A.5) implies $L^{ii}(k) > 0$, $i \neq 0$, a condition we will use to bound the fluctuation. If we take $j = 0$, eq. (A.5) means

$$L^{ii}(k) + L^{00}(k) - 2L^{i0}(k) > 0 \tag{A.8}$$

Since ρ_{xy} is normalized. $L^{00}(k) = L^{i0}(k) = 0$. Thus $L^{ii}(k) > 0$.

Now we calculate the partition function in $(k > 2)$ replica with an arbitrary boundary condition. Using permutation symmetry between vertices in the complete graph, eq. (A.3) can be rewritten as

$$\overline{Z_1^{(k)}} = \sum_{\{n_i\},\{m_i\}} e^{-A(n_i,m_i)} \frac{V_b!}{n_0! n_1! \cdots n_{k!-1}!} \frac{V_B!}{m_0! m_1! \cdots m_{k!-1}!} \tag{A.9}$$

$$A(n_i, m_i) = \sum_{i>j} J^{ij}(n_i + m_i)(n_j + m_j) + \sum_i \frac{J^{ii}}{2}(n_i + m_i)(n_i + m_i - 1) + \sum_i B^i m_i$$

with

$$J^{ij} = -\log \operatorname{tr}\left(\rho_{xy}^{\otimes k} g_x^i g_y^j\right) \qquad B^i = -\log \operatorname{tr}\left(\rho_{\text{EPR}}^{\otimes k} g_x^i h\right) \qquad L^{ij} = (J^{i0} + J^{0j} - J^{ij})/2$$

$$\sum_i n_i = V_b \qquad\qquad \sum_i m_i = V_B$$

where $n_i(m_i)$ is the number of bulk(boundary) points occupied by the group element g^i; $V_b(V_B)$ is the total number of bulk(boundary) points; $h_X = h$ fixes the boundary condition.

Then we replace $n_0 = V_b - \sum_{i\geq 1} n_i$, $m_0 = V_B - \sum_{i\geq 1} m_i$. Since $J^{00} = 0$, we have

$$A(n_i, m_i) = \sum_{i>j\geq 1} J^{ij}(n_i + m_i)(n_j + m_j) + \sum_{i\geq 1} J^{i0}(n_i + m_i)\left(V_b + V_B - \sum_{j\geq 1}(n_j + m_j)\right)$$

$$+ \sum_{i\geq 1} \frac{J^{ii}}{2}(n_i + m_i)(n_i + m_i - 1) + \sum_i B^i m_i$$

$$= \sum_{i,j \geq 1} -(n_i + m_i) L^{ij} (n_j + m_j) + \sum_{i \geq 1} \left((V_b + V_B) L^{ii} + (V_b + V_B - 1) \frac{J^{ii}}{2} \right) n_i$$

$$+ \sum_{i \geq 1} \left((V_b + V_B) L^{ii} + (V_b + V_B - 1) \frac{J^{ii}}{2} + B^i - B^0 \right) m_i + B^0 V_B \qquad \text{(A.10)}$$

In the large V_b, V_B limit, we treat n_i and m_i as continuous variables to decide where $F(n_i, m_i) \equiv -A(n_i, m_i) - \sum_i \log n_i! - \sum_i \log m_i!$ reaches its maximum. We use Stirling formula and calculate the second derivatives of this function

$$M = \begin{bmatrix} M_1 & M_2 \\ M_2 & M_3 \end{bmatrix} \qquad \text{(A.11)}$$

$$M_1^{ij} = \frac{\partial^2}{\partial n_i \partial n_j} F(n_i, m_j) = 2L^{ij} - \frac{\delta_{ij}}{n_i} - \frac{1}{n_0}$$

$$M_2^{ij} = \frac{\partial^2}{\partial n_i \partial m_j} F(n_i, m_j) = 2L^{ij}$$

$$M_3^{ij} = \frac{\partial^2}{\partial m_i \partial m_j} F(n_i, m_j) = 2L^{ij} - \frac{\delta_{ij}}{m_i} - \frac{1}{m_0}$$

Now we show that F does not have local minimum away from the corners of the parameter space. A local minimum requires M to be a negative definite matrix, so to prove that F does not have local minimum one just needs to show that M is not negative definite anywhere away from the corners. A corner of the parameter space (labeled by n_i/V_b, m_i/V_B) is defined by having one $n_i = V_b$, $m_j = V_B$ and all other numbers vanishing. Therefore for any point away from these corners, there are either two numbers n_i, n_j of order V_b, or two numbers m_i, m_j of order V_B. Let's assume there are n_i, n_j of order V_b since the discussion with m_i, m_j is exactly in parallel. This includes the following two cases:

- If n_0 is of $O(1)$, then there are two n_i, n_j with $i, j > 0$ of order $O(V_b)$. Define a vector $\vec{v}$ whose ith element is 1, jth element is -1 and all others are 0. Obviously,

$$v^T M v = 2 \left(L^{ii} + L^{jj} - 2L^{ij} \right) - \frac{1}{n_i} - \frac{1}{n_j} \qquad \text{(A.12)}$$

Since $L^{ii} + L^{jj} - 2L^{ij} > 0$, and n_i, n_j are $O(V_b)$, $v^T M v > 0$. So M is not negative definite and there is no local maximum in this case away from the corners.

- If n_0 is of $O(V_b)$, then there is at least another n_i being $O(V_b)$. We choose $\vec{v}$ whose only non-zero element is 1 at the ith element. Thus

$$v^T M v = 2L^{ii} - \frac{1}{n_i} - \frac{1}{n_0} \qquad \text{(A.13)}$$

Since $L^{ii} > 0$ is $O(1)$ and n_0, n_i is $O(V_b)$, $v^T M v > 0$.

Therefore we conclude that eq. (A.5) is the sufficient condition that guarantees $F(n_i, m_i)$ does not have local minimum away from the corners.

The next step is to compare the value of $F(n_i, m_i)$ of each corner solution and bound the near corner solutions. The corner solutions are categorized as

- S_{n_0,m_0}: $n_0 = V_b$, $m_0 = V_B$,
$$F(S_{n_0,m_0}) = -B^0 V_B \tag{A.14}$$

- S_{n_i,m_0}: $n_i = V_b$, $i \geq 1$, $m_0 = V_B$,
$$F(S_{n_i,m_0}) = -B^0 V_B - V_b V_B L^{ii} - (V-1)\frac{J^{ii}V_b}{2} \tag{A.15}$$

- S_{n_0,m_j}: $n_0 = V_b$, $m_j = V_B$, $j \geq 1$,
$$F(S_{n_0,m_j}) = -B^j V_B - V_b V_B L^{jj} - (V-1)\frac{J^{jj}V_B}{2} \tag{A.16}$$

- S_{n_i,m_j}: $n_i = V_b$, $m_j = V_B$, $i,j \geq 1$,
$$F(S_{n_i,m_j}) = -B^j V_B - V_b V_B \left(L^{ii} + L^{jj} - 2L^{ij}\right) - (V-1)\frac{J^{ii}V_b + J^{jj}V_B}{2} \tag{A.17}$$

Firstly, we notice that $F(S_{n_0,m_0}) \gg F(S_{n_i,m_0})$ is always true, because $L^{ii} > 0$ is assumed and $J^{ii} = \log D_L \left(k - \chi(g^i)\right) > 0$, where $\chi(g)$ denotes the number of cycles in a permutation g.

Secondly,
$$
\begin{aligned}
&F(S_{n_0,m_0}) - F(S_{n_0,m_j}) \\
&= V_B \log D \left(k - \chi((g^j)^{-1}h) - (k - \chi(h))\right) + V_B V_b L^{ii} + (V-1)\frac{J^{jj}V_B}{2} \\
&\geq -V_B \log D \left(k - \chi((g^j)^{-1})\right) + (V-1)\frac{V_B}{2} \log D_L \left(k - \chi((g^j)^{-1})\right) \tag{A.18}
\end{aligned}
$$

In the inequality, we use $L^{ii} > 0$, and the triangle inequality of $d(g,h) \equiv k - \chi(g^{-1}h)$, which is equal to the minimal number of transpositions (i.e., permutations that exchange only two indices) required to write a permutation $g^{-1}h$. $d(g,h)$ defines a distance on S_k, which satisfies the triangle inequality $d(g,I) + d(I,h) \geq d(g,h)$ [23]. Thus eq. (A.4) $(V-1)\log D_L \gg 2 \log D$ is a sufficient condition for $F(S_{n_0,m_0}) \gg F(S_{n_0,m_j})$.

Thirdly,
$$
\begin{aligned}
&F(S_{n_0,m_0}) - F(S_{n_i,m_j}) \\
&= V_B \log D \left(k - \chi((g^j)^{-1}g^\partial) - (k - \chi(g^\partial))\right) + V_B V_b (L^{ii} + L^{jj} - 2L^{ij}) \\
&\quad + (V-1)\frac{J^{ii}V_b + J^{jj}V_B}{2} \\
&> V_B \log D \left(k - \chi((g^j)^{-1}g^\partial) - (k - \chi(g^\partial))\right) + (V-1)\frac{V_B}{2} \log D_L \left(k - \chi((g^j)^{-1})\right) \\
&\geq -V_B \log D \left(k - \chi((g^j)^{-1})\right) + (V-1)\frac{V_B}{2} \log D_L \left(k - \chi((g^j)^{-1})\right) \tag{A.19}
\end{aligned}
$$

where in the first inequality, we use $J^{ii} > 0$ and $L^{ii} + L^{jj} - 2L^{ij} > 0$. In the second inequality, we use the triangle inequality of $k - \chi((g^i)^{-1}g^j)$ again. Thus if eq. (A.4) holds, we also have $F(S_{n_0,m_0}) \gg F(S_{n_i,m_j})$.

In fact, we can make tighter bounds in $F(S_{n_0,m_0}) - F(S_{n_i,m_j})$ and $F(S_{n_0,m_0}) - F(S_{n_0,m_j})$ if we do not simply discard L^{ii} or $L^{ii} + L^{jj} - 2L^{ij}$. However, using condition eq. (A.4) has the advantage that it does not depend on k and the details of the link state.

Finally, we can bound $\overline{Z_i^{(k)}}$ by analyzing the configurations near the corners. We have shown that when eq. (A.4) and eq. (A.5) are satisfied, all other corner solutions are exponentially small compared with the dominating corner S_{n_0,m_0}, and the exponent is suppressed by $-\frac{k-\chi(g^j)}{2}V_B((V-1)\log D_L - 2\log D)$. Thus the next biggest configuration is at the neighborhood of the corner solution S_{n_0,m_0}. In fact we can bound all configurations that are finite distance away from S_{n_0,m_0} by $C \cdot \exp\left[-\frac{(V-1)\log D_L - 2\log D}{2}\right]$, where C is a $O(1)$ number. Thus we obtain that

$$\overline{Z_i^{(k)}} \leq e^{-B^0 V_B}\left(1 + C(V_B V_b)^{k!-1}\exp\left[-\frac{(V-1)\log D_L - 2\log D}{2}\right]\right) \qquad (A.20)$$

where $(V_B V_b)^{k!-1}$ is the total number of configurations of $F(n_i, m_j)$.

We conclude that if eq. (A.4), (A.5) are satisfied, the fluctuation is controlled and all higher Renyi entropies are close to $V_B \log D$. Thus there is an isometry from the boundary to the bulk.

A.2 A sufficient condition for eq. (A.5)

In this section, we provide a sufficient condition that deduces eq. (A.5), which helps to clarify what density matrices satisfy this equation. In a basis $|\alpha_x\rangle = \prod_{s=1}^k |\alpha_x^k\rangle$ of the k-copied Hilbert space, density operators and permutation operators are written as

$$\rho_{xy}^{\otimes k} = \left(\rho_{xy}^{\otimes k}\right)_{\alpha,\beta,\gamma,\delta}(|\alpha_x\rangle \otimes |\beta_y\rangle)(\langle\gamma_x| \otimes \langle\delta_y|) \qquad (A.21)$$

$$g^j = (g^j)_{\alpha,\beta}|\alpha\rangle\langle\beta| \qquad (A.22)$$

One can rearrage the indices and write

$$\text{Tr}\left[\rho_{xy}^{\otimes k}g_x^i g_y^j\right] = (g^i)_{\gamma,\alpha}\left(\rho_{xy}^{\otimes k}\right)_{\alpha,\beta,\gamma,\delta}(g^j)_{\delta,\beta} = \langle g^i|\tilde{\rho}_{xy}^{\otimes k}|g^j\rangle \qquad (A.23)$$

$$\tilde{\rho}_{xy}^{\otimes k} \equiv \left(\rho_{xy}^{\otimes k}\right)_{\alpha,\beta,\gamma,\delta}(|\alpha_x\rangle \otimes |\gamma_x\rangle)(\langle\beta_y| \otimes \langle\delta_y|) \qquad (A.24)$$

$$|g^j\rangle \equiv (g^j)_{\alpha,\beta}|\alpha\rangle \otimes |\beta\rangle, \qquad \langle g^i| \equiv (g^i)_{\alpha,\beta}\langle\alpha| \otimes \langle\beta| \qquad (A.25)$$

where in the last step, we have used the fact that the matrix elements $g_{\alpha,\beta}^i$ in the product basis are real. In this representation, $\text{Tr}\left[\rho_{xy}^{\otimes k}g_x^i g_y^j\right]$ becomes an inner product between states $|g^i\rangle, |g^j\rangle$ with metric $\tilde{\rho}_{xy}^{\otimes k}$. Therefore eq. (A.5) follows from Cauchy-Schwarz inequality if $\tilde{\rho}_{xy}^{\otimes k}$ is Hermitian and positive semi-definite for all k. Thus we conclude that a sufficient but not necessary condition for eq. (A.5) is that $\tilde{\rho}_{xy}$ is Hermitian and positive semi-definite. This condition is not necessary since eq. (A.5) is only required for permutation operators and does not need to hold for general operators.

A.3 An explicit example of states $|a_{xy}\rangle$

In this section, we provide an explicit example of link states $|a_{xy}\rangle$ and prove that condition (eq. (3.17) is satisfied. We define the state $|J\rangle$ as a SU(2) singlet formed by two spins each carrying spin J representation:

$$|J\rangle \equiv \sum_M \frac{(-)^{J-M}}{\sqrt{2J+1}} |J, M; J, -M\rangle \tag{A.26}$$

with $J = 0, 1, \ldots, D_L - 1$ labeling the link states. The Hilbert space of each site is a direct sum of different representations $\mathbb{H}_x = \oplus_{J=0}^{D_L-1} \mathbb{H}_J$. States with different J obviously are orthogonal. (A subtlety is that the entropy of state $|J\rangle$ is $\log(2J+1)$, so that we should think the link variable $a \propto \log(2J+1)$ if we still want a to label the entropy across the link. This does not affect any discussion here.) The density matrix ρ_{xy} is given by

$$\rho_{xy} \equiv \frac{1}{D_L - 1} \sum_{J=1}^{D_L} |J\rangle\langle J| \tag{A.27}$$

If one directly obtains $\tilde{\rho}_{xy}$ in eq. (A.24) for ρ_{xy}, the resulting ρ_{xy} is Hermitian but not positive semi-definite. However, we can prove ρ_{xy} satisfies condition (A.5) by defining a unitary operator on the y site

$$u_y = \sum_{J,M} (-1)^M |J, -M\rangle \langle J, M| \tag{A.28}$$

The density matrix in the new basis is

$$\sigma_{xy} \equiv u_y \rho_{xy} u_y^\dagger = \frac{1}{D_L - 1} \sum_{J=0}^{D_L-1} \frac{1}{2J+1} \sum_{M,N} |J, M; J, M\rangle \langle J, N; J, N| \tag{A.29}$$

Since $u_y^{\otimes k}$ commutes with permutation operators g_y^i, we have $\text{Tr}\left[\sigma_{xy}^{\otimes k} g_x^i g_y^j\right] = \text{Tr}\left[\rho_{xy}^{\otimes k} g_x^i g_y^j\right]$. For σ_{xy}, the corresponding operator $\tilde{\sigma}_{xy}$ defined in eq. (A.24) is

$$\tilde{\sigma}_{xy} = \frac{1}{D_L - 1} \sum_{J=0}^{D_L-1} \frac{1}{2J+1} \sum_{M,N} |J, M; J, N\rangle \langle J, M; J, N| = \oplus_{J=0}^{D_L-1} \frac{1}{(D_L-1)(2J+1)} \mathbb{I}_J \tag{A.30}$$

with $\mathbb{I}_J$ an identity matrix of the size $(2J+1)^2 \times (2J+1)^2$. Obviously $\tilde{\sigma}_{xy}$ is diagonal and positive definite, so that we prove σ_{xy} and therefore ρ_{xy} satisfy eq. (A.5).

References

[1] E. Witten, *Anti-de Sitter space and holography*, *Adv. Theor. Math. Phys.* **2** (1998) 253 [hep-th/9802150] [INSPIRE].

[2] S.S. Gubser, I.R. Klebanov and A.M. Polyakov, *Gauge theory correlators from noncritical string theory*, *Phys. Lett.* **B 428** (1998) 105 [hep-th/9802109] [INSPIRE].

[3] J.M. Maldacena, *The large-N limit of superconformal field theories and supergravity*, *Int. J. Theor. Phys.* **38** (1999) 1113 [hep-th/9711200] [INSPIRE].

[4] S. Ryu and T. Takayanagi, *Holographic derivation of entanglement entropy from AdS/CFT*, *Phys. Rev. Lett.* **96** (2006) 181602 [hep-th/0603001] [INSPIRE].

[5] V.E. Hubeny, M. Rangamani and T. Takayanagi, *A covariant holographic entanglement entropy proposal*, *JHEP* **07** (2007) 062 [arXiv:0705.0016] [INSPIRE].

[6] T. Faulkner, A. Lewkowycz and J. Maldacena, *Quantum corrections to holographic entanglement entropy*, *JHEP* **11** (2013) 074 [arXiv:1307.2892] [INSPIRE].

[7] X. Dong, A. Lewkowycz and M. Rangamani, *Deriving covariant holographic entanglement*, *JHEP* **11** (2016) 028 [arXiv:1607.07506] [INSPIRE].

[8] X. Dong, *The gravity dual of Rényi entropy*, *Nature Commun.* **7** (2016) 12472.

[9] B. Swingle, *Entanglement Renormalization and Holography*, *Phys. Rev.* **D 86** (2012) 065007 [arXiv:0905.1317] [INSPIRE].

[10] B. Swingle, *Constructing holographic spacetimes using entanglement renormalization*, arXiv:1209.3304 [INSPIRE].

[11] S.R. White, *Density matrix formulation for quantum renormalization groups*, *Phys. Rev. Lett.* **69** (1992) 2863 [INSPIRE].

[12] S.R. White, *Density-matrix algorithms for quantum renormalization groups*, *Phys. Rev.* **B 48** (1993) 10345 [INSPIRE].

[13] F. Verstraete, D. Porras and J.I. Cirac, *Density Matrix Renormalization Group and Periodic Boundary Conditions: A Quantum Information Perspective*, *Phys. Rev. Lett.* **93** (2004) 227205 [INSPIRE].

[14] F. Verstraete and J.I. Cirac, *Renormalization algorithms for quantum-many body systems in two and higher dimensions*, cond-mat/0407066 [INSPIRE].

[15] G. Vidal, *Class of Quantum Many-Body States That Can Be Efficiently Simulated*, *Phys. Rev. Lett.* **101** (2008) 110501 [INSPIRE].

[16] Z.-C. Gu and X.-G. Wen, *Tensor-Entanglement-Filtering Renormalization Approach and Symmetry Protected Topological Order*, *Phys. Rev.* **B 80** (2009) 155131 [arXiv:0903.1069] [INSPIRE].

[17] J.J. Heckman and C. Vafa, *F-theory, GUTs and the Weak Scale*, *JHEP* **09** (2009) 079 [arXiv:0809.1098] [INSPIRE].

[18] S. El-Showk and K. Papadodimas, *Emergent Spacetime and Holographic CFTs*, *JHEP* **10** (2012) 106 [arXiv:1101.4163] [INSPIRE].

[19] P. Hayden, M. Headrick and A. Maloney, *Holographic Mutual Information is Monogamous*, *Phys. Rev.* **D 87** (2013) 046003 [arXiv:1107.2940] [INSPIRE].

[20] X.-L. Qi, *Exact holographic mapping and emergent space-time geometry*, arXiv:1309.6282 [INSPIRE].

[21] F. Pastawski, B. Yoshida, D. Harlow and J. Preskill, *Holographic quantum error-correcting codes: Toy models for the bulk/boundary correspondence*, *JHEP* **06** (2015) 149 [arXiv:1503.06237] [INSPIRE].

[22] Z. Yang, P. Hayden and X.-L. Qi, *Bidirectional holographic codes and sub-AdS locality*, *JHEP* **01** (2016) 175 [arXiv:1510.03784] [InSPIRE].

[23] P. Hayden, S. Nezami, X.-L. Qi, N. Thomas, M. Walter and Z. Yang, *Holographic duality from random tensor networks*, *JHEP* **11** (2016) 009 [arXiv:1601.01694] [InSPIRE].

[24] A. Almheiri, X. Dong and D. Harlow, *Bulk Locality and Quantum Error Correction in AdS/CFT*, *JHEP* **04** (2015) 163 [arXiv:1411.7041] [InSPIRE].

[25] X. Dong, *Shape Dependence of Holographic Rényi Entropy in Conformal Field Theories*, *Phys. Rev. Lett.* **116** (2016) 251602 [arXiv:1602.08493] [InSPIRE].

[26] W. Donnelly, B. Michel, D. Marolf and J. Wien, *Living on the Edge: A Toy Model for Holographic Reconstruction of Algebras with Centers*, *JHEP* **04** (2017) 093 [arXiv:1611.05841] [InSPIRE].

[27] B.S. DeWitt, *Quantum Theory of Gravity. 1. The Canonical Theory*, *Phys. Rev.* **160** (1967) 1113 [InSPIRE].

[28] D. Harlow, *The Ryu-Takayanagi Formula from Quantum Error Correction*, *Commun. Math. Phys.* **354** (2017) 865 [arXiv:1607.03901] [InSPIRE].

[29] K. Papadodimas and S. Raju, *An Infalling Observer in AdS/CFT*, *JHEP* **10** (2013) 212 [arXiv:1211.6767] [InSPIRE].

[30] D. Harlow, *Aspects of the Papadodimas-Raju Proposal for the Black Hole Interior*, *JHEP* **11** (2014) 055 [arXiv:1405.1995] [InSPIRE].

[31] N. Lashkari, M.B. McDermott and M. Van Raamsdonk, *Gravitational dynamics from entanglement 'thermodynamics'*, *JHEP* **04** (2014) 195 [arXiv:1308.3716] [InSPIRE].

[32] T. Faulkner, M. Guica, T. Hartman, R.C. Myers and M. Van Raamsdonk, *Gravitation from Entanglement in Holographic CFTs*, *JHEP* **03** (2014) 051 [arXiv:1312.7856] [InSPIRE].

[33] B. Swingle and M. Van Raamsdonk, *Universality of Gravity from Entanglement*, arXiv:1405.2933 [InSPIRE].

[34] T. Jacobson, *Entanglement Equilibrium and the Einstein Equation*, *Phys. Rev. Lett.* **116** (2016) 201101 [arXiv:1505.04753] [InSPIRE].

[35] S. Lloyd, *The quantum geometric limit*, arXiv:1206.6559 [InSPIRE].

[36] E.P. Verlinde, *On the Origin of Gravity and the Laws of Newton*, *JHEP* **04** (2011) 029 [arXiv:1001.0785] [InSPIRE].

[37] J.B. Hartle and S.W. Hawking, *Wave Function of the Universe*, *Phys. Rev.* **D 28** (1983) 2960 [InSPIRE].

[38] A.A. Deriglazov, *Poincaré covariant mechanics on noncommutative space*, *JHEP* **03** (2003) 021 [hep-th/0211105] [InSPIRE].

[39] D.L. Jafferis, *Bulk reconstruction and the Hartle-Hawking wavefunction*, arXiv:1703.01519 [InSPIRE].

[40] Y. Nomura, N. Salzetta, F. Sanches and S.J. Weinberg, *Toward a Holographic Theory for General Spacetimes*, *Phys. Rev.* **D 95** (2017) 086002 [arXiv:1611.02702] [InSPIRE].

[41] Y. Nomura, N. Salzetta, F. Sanches and S.J. Weinberg, *Spacetime Equals Entanglement*, *Phys. Lett.* **B 763** (2016) 370 [arXiv:1607.02508] [InSPIRE].